The Fluctuating Longshore Pressure Gradient on the Pacific Northwest Shelf: A Dynamical Analysis[1]

BARBARA M. HICKEY

School of Oceanography, University of Washington, Seattle, WA 98195

(Manuscript received 28 May 1983, in final form 8 September 1983)

ABSTRACT

The majority of papers on Pacific Northwest shelf dynamics have emphasized the relationship between longshore wind stress τ_s and longshore velocity v. However, attempts to illustrate a balance of momentum in the longshore direction have not been encouraging: τ_s/H (where H is water depth) has insufficient magnitude to balance the vertically averaged longshore acceleration V_t, at least during summer. In this paper it is demonstrated that the missing momentum is provided by the longshore pressure gradient force $-p_y$. The pressure gradient was estimated using tide gauge and atmospheric pressure data at stations separated by roughly 400 km. Seasonal and long-term means from Hickey and Pola and, in some cases, nonseasonal monthly anomalies from Enfield and Allen were added to the sum of the tide gauge and atmospheric pressure data to form time series of total subsurface pressure. The pressure data were multiplied by an offshore decay factor to simulate coastal trapping.

The analysis was performed during four separate two-month periods, spanning four years and two seasons. In each case, inclusion of p_y in the vertically averaged longshore momentum equation improved the balance with computed acceleration. Some events were forced primarily by τ_s/H, others by $-p_y$. However, during some extended periods, one or the other force dominated; for example, during summer 1978, $-p_y$ provided almost all the force to balance the acceleration. During every period, V_t and $-p_y$ were significantly coherent at the 95% level and the phase difference between the time series was close to zero at most frequencies, as expected for a barotropic wave-like disturbance such as a first mode hybrid coastal trapped wave in this region. The pressure field at frequencies ≤ 0.3 cpd was consistent during all periods with northward propagation at speeds on the order of the free first mode coastal trapped wave or 50–200% faster. However, individual events during periods of weak local winds were observed to propagate through the region at the free first mode wave speed; also, p_y was only weakly correlated to local τ_s. Thus it appears that whereas the local pressure field is significantly affected by local wind forcing, the pressure gradient field is generated primarily nonlocally. At the extremely energetic higher frequencies (0.35–0.50 cycles per day) during winter, first mode freely propagating coastal trapped waves do not appear to be as important to the dynamics.

1. Introduction

A strong relationship between the longshore component of current (v) and the longshore component of local wind stress (τ_s) in the Pacific Northwest on event (<1 cycle per day) scales is widely acknowledged (Smith, 1974; Kundu *et al.* 1975; Huyer *et al.*, 1975; Hickey, 1981). The observed relationship is generally based on correlation or coherence and phase analyses between v and τ_s. In a recent attempt to demonstrate a balance between vertically integrated longshore acceleration and longshore wind stress, the conclusion is that the amplitude of fluctuations in longshore wind stress is too small to balance vertically integrated longshore acceleration fluctuations (Allen and Smith, 1981). An obvious candidate for providing the additional required momentum is the longshore pressure gradient force.

When this study began, no one had yet attempted to calculate explicitly the contributions to the mean or fluctuating current by the longshore pressure gradient. The reasons for this were twofold: first, although a relative subsurface pressure gradient could be readily calculated from differences between tide gauge plus atmospheric pressure data at two stations, the mean gradient over any record length was unknown. Second, investigators believed that the signal-to-noise ratio would be small. Hence, the longshore pressure gradient term in the equation of motion was never prescribed, preventing unequivocable determination of the wave-like nature of the coastal response. Allen and Smith (1981) subsequently attempted to estimate this term, but their results were not encouraging (see Section 6). Specifically, the longshore pressure gradient was positively, rather than negatively correlated with acceleration, the opposite of what would be expected for the low frequency free waves suggested by Wang and Mooers (1977) for the period investigated.

The present study demonstrates that the contribution to the longshore acceleration by the large-scale long-

[1] Contribution No. 1364 from the School of Oceanography, University of Washington, Seattle, WA 98195.

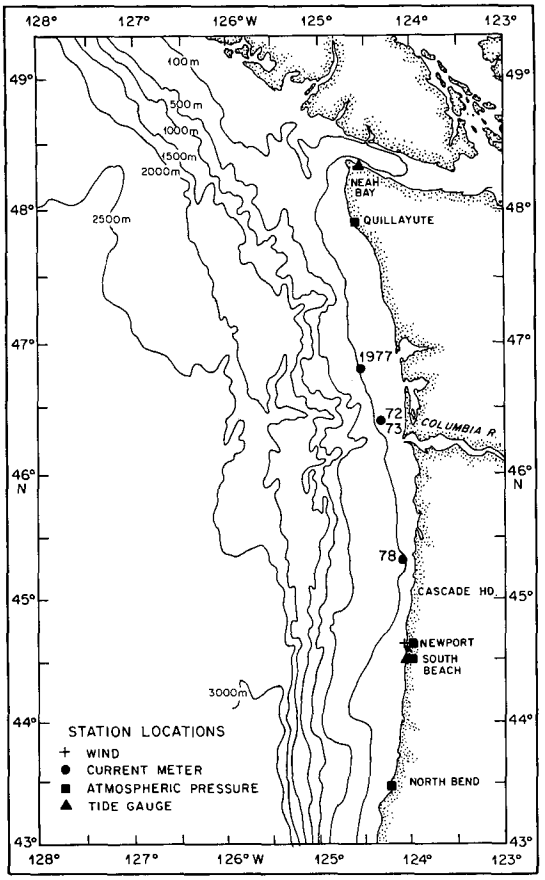

FIG. 1. Locations of current meter moorings and sea level, wind and atmospheric pressure stations and their physical setting.

shore pressure gradient can be adequately determined from tide gauge and atmospheric pressure data. The working hypothesis is that longshore wind stress and longshore pressure gradient force together are the principal forces accelerating the water column. This hypothesis is tested during four separate two-month periods, spanning four years and two seasons: winter of 1973 and 1977 and summer of 1972 and 1978.

The philosophy of the study is to determine the extent to which the various measurable forces and sums of forces contribute to the observed longshore acceleration time series. Goodness of fit is tested by time series inspection, energy level comparisons and coherence and phase estimates. Results of these analyses are then examined in the context of wave dynamics.

2. The dataset

The dataset includes current observations at mid-shelf locations, wind speed and direction measured at the coast and sea level height and atmospheric pressure at stations along the Oregon–Washington coast (Fig. 1). Mooring parameters are given in Table 1. All current data were obtained with Aanderaa RCM-4 or RCM-5 current meters sampling at 10 or 20 minute intervals. The data were filtered to obtain hourly values of current speed and direction. Since the flow generally follows the local isobaths (Huyer *et al.*, 1978; Kundu and Allen, 1976), a local Cartesian reference frame, with y positive northward along the isobaths, x positive onshore and z positive downward, is used.

Hourly sea level data were obtained for Neah Bay, Washington and South Beach, Oregon. Atmospheric pressure data were obtained for Quillayute, Washington (all years); South Beach, Oregon (1972, 1973), Newport, Oregon (1977) and North Bend, Oregon (1978). The South Beach station (both sea level and atmospheric pressure) is maintained by Oregon State University. The Neah Bay sea level station and the Quillayute, North Bend and Newport atmospheric pressure stations are maintained by the National Ocean Survey (sea level) and the National Climatic Center (atmospheric pressure). The wind data were obtained as hourly speed and direction from the Newport wind station operated by Oregon State University.

The hourly sea level and current data were low-pass filtered with a symmetrical cosine filter with a half-power point of 0.6 cycles per day (cpd). These time series were then decimated to six-hourly values. Surface and bottom stress were calculated from hourly data, then filtered and decimated to six-hourly values in the same manner as the other data sets.

3. Methods and assumptions

The homogenous, linear, vertically averaged longshore momentum equation is

$$V_t = T_s - p_y - T_b - fU, \qquad (1)$$

where t is time, f is the Coriolis parameter, V and U are the along- and cross-isobath vertically averaged components of velocity (referred to as longshore and cross-shore components respectively), p_y is the longshore pressure gradient divided by water density, ρ_w (=1.0) and T_s and T_b are the longshore components

TABLE 1. Mooring parameters.

Year	Period	Latitude	Longitude	Bottom depth (m)	Meter depth (m)	Record length (days)
1972	July 21–Sept 15	46°24.8'N	124°20.0'W	78	50, 71	56
1973	Jan 9–March 5	46°24.8'N	124°20.0'W	78	50, 71	56
1977	Jan 12–March 8	46°49.5'N	124°32.5'W	100	25, 80	56
1978	Aug 15–Oct 10	45°20.1'N	124°08.8'W	110	92	56

of surface and bottom stress divided by $\rho_w H$, where H is water depth. An *in situ* test of this equation requires many assumptions with respect to both applicability of particular datasets and the parameterization of specific terms. The specific assumptions and parameterizations used in this analysis are detailed below.

Bottom stress was calculated using a quadratic stress law

$$T_b = \left(\frac{C_d}{H}\right)|\mathbf{v}_b|v_b$$

where $\mathbf{v}_b = (u_b, v_b)$ is the near-bottom current vector and C_d is a drag coefficient. The near-bottom current meter was located 7, 7, 20 and 18 m off the bottom in 1972, 1973, 1977 and 1978 respectively. The drag coefficient used is a speed variable quadratic function [$C_d = (2.33 - 0.053|\mathbf{v}_b| + 0.00036|\mathbf{v}_b|^2) \times 10^{-3}$] ($\mathbf{v}_b$ in cm s^{-1}) determined for Pacific Northwest shelf sediment and bottom roughness conditions (see Kachel, 1980). Differences between drag coefficients calculated for distances 7 and 20 m above the bottom were negligible. The Kachel drag coefficient includes the effects of near-bottom stratification caused by sediment resuspension. The constant drag coefficient of 1.3×10^{-3} that has been used by many investigators (e.g., Allen and Smith, 1981) is attained at a speed of 19 cm s^{-1}. Under winter storm conditions when speeds in excess of 40 cm s^{-1} are common, the variable drag coefficient reduces the observed stress by a factor of 2 or more over that obtained with a constant drag coefficient of 1.3×10^{-3}. Effects of surface waves on C_d, which are probably important during winter, are not included in the formulation since specific wave conditions during individual events are unknown.

Surface stress was calculated using

$$T_s = \left(\frac{\rho_a C_s}{\rho_w H}\right)|\mathbf{w}|w_y,$$

where $\mathbf{w} = (w_x, w_y)$ is the wind vector, ρ_a the density of air and C_s the surface drag coefficient calculated according to Large and Pond (1981). For wind speeds less than 11 m s^{-1}, $C_s = 1.2 \times 10^{-3}$; for wind speeds greater than or equal to 11 m s^{-1}, $C_s = (0.49 + 0.065|\mathbf{w}_{10}|) \times 10^{-3}$, where $|\mathbf{w}_{10}|$ is the wind speed (in m s^{-1}) at a height of 10 m. This drag coefficient was applied directly to Newport wind data, which is obtained at a height of 9 m above the Newport jetty (Pittock *et al.*, 1982). To obtain a correction factor for the land-to-ocean gradient in wind speed, mid-shelf buoy wind stress data off Oregon given by Halpern (1976) were compared by linear regression with simultaneous Newport wind stress data given by Kundu and Allen (1976). The data, which were taken during summer, suggest that the offshore wind exceeds that measured at the shore by a factor of ~1.3. No similar data are available for the winter season when the wind generally comes from the south rather than from the north. However, field experience suggests that a coast-to-ocean wind gradient does exist. The Newport wind magnitude was therefore increased by a factor of 1.3 in both seasons. Note that the gradient in stress will be larger in winter than in summer, a result of the variable drag coefficient. Wind amplification was not included in summer 1972, when current meter data were obtained off Washington rather than Oregon (see Section 6).

The longshore acceleration V_t was calculated with a central difference scheme:

$$V_t^i = \frac{V^{i+1} - V^{i-1}}{2\Delta t},$$

where Δt = 6 h. Velocity data are not available in the surface Ekman layer for any of the periods investigated; nor are they available at regularly spaced intervals throughout the interior water column; during some periods data are available only at a single depth. Therefore, the vertical average of velocity was estimated from single depth mid-water column data. The data are either well outside (3 cases) or at the outer edge of (1977 only) the expected frictional bottom boundary layer (Kundu, 1977; Huyer *et al.*, 1978). The error associated with using single depth mid-water column data to represent the vertical average is small (<20%) since the fluctuating longshore velocity in the Pacific Northwest is primarily barotropic at mid-shelf locations (Smith *et al.*, 1976, for the Washington shelf; Huyer *et al.*, 1978, for the Oregon shelf).

The subsurface longshore pressure gradient (p_y) was obtained by forming the gradient in *de-meaned* tide gauge data between two stations roughly 400 km apart and adding this to the gradient in *de-meaned* atmospheric pressure data (converted from mb to cm of water). The 400 km spacing limits the scale of features that can be resolved. In particular, wave-like disturbances with scales much smaller than 1600 km will not be adequately sampled. Seasonal monthly mean subsurface pressure (Hickey and Pola, 1983) and non-seasonal monthly subsurface pressure anomalies (Enfield and Allen, 1980; for 1972 and 1973 only) were added to the data. The seasonal means of Hickey and Pola include long-term mean 0/500 db steric height data that Reid and Mantyla (1976) extrapolated to the coast. The magnitude of the long-term mean pressure gradient term is on the order of 0.5×10^{-4} cm s^{-2}, whereas event-scale fluctuations are on the order of 1.5×10^{-4} cm s^{-2}. Finally, a linear offshore decay of the longshore pressure gradient was applied, consistent with results of coastal trapped wave models for the Oregon shelf (Brink, 1982) (a factor of 0.7–0.8 at mid-shelf).

The remaining term in (1), fU was an enigma in Allen and Smith (1981), which is the only study in which it has actually been computed. The expectation

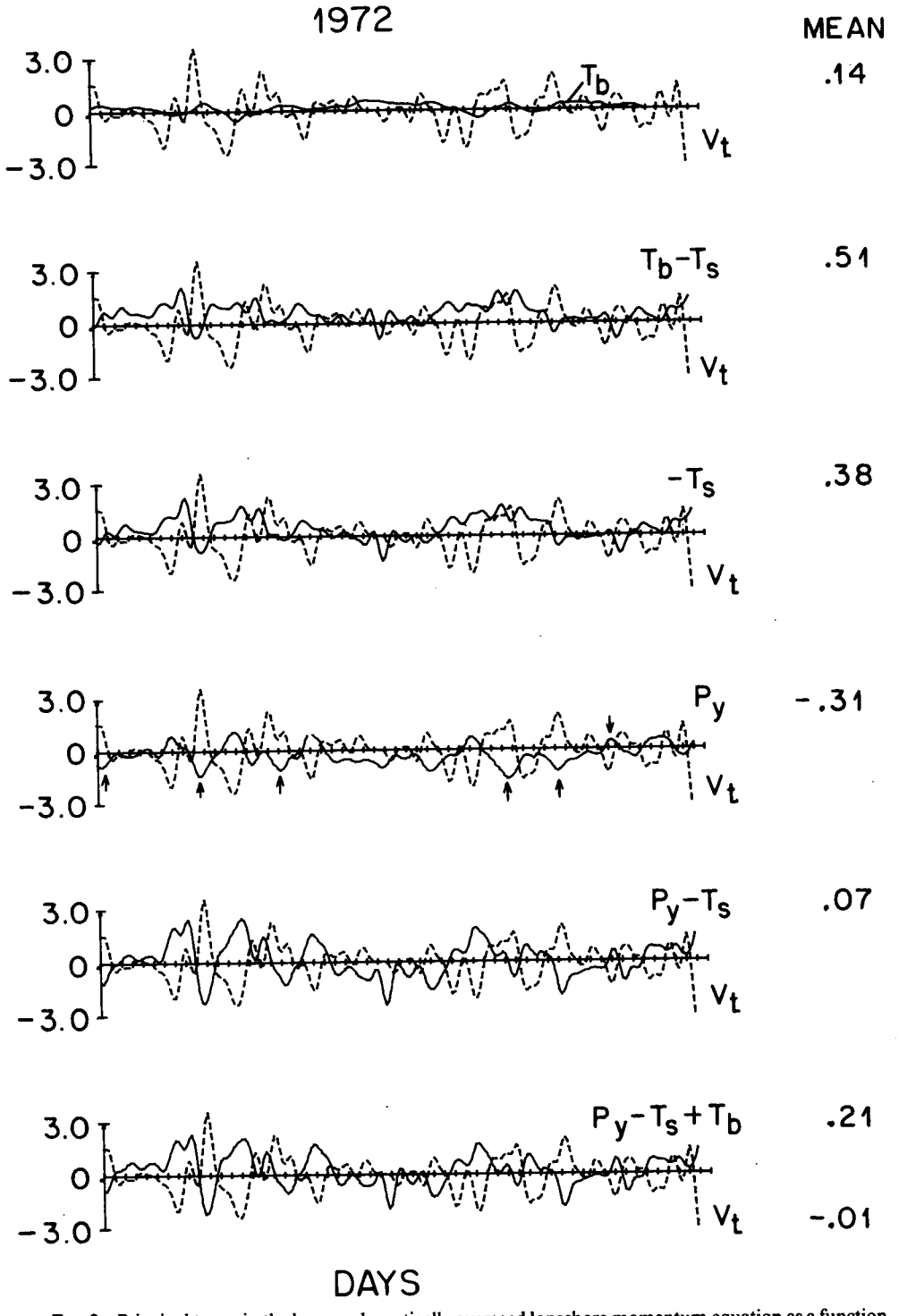

FIG. 2a. Principal terms in the large-scale vertically averaged longshore momentum equation as a function of time during summer 1972. A mirror image between a pair of plots indicates a perfect balance of momentum. Vertical arrows are used to indicate periods when p_y is particularly significant to the balance. Units are 10^{-4} cm s^{-2}. The mean of each series is given on the right.

would be for fU to approach zero if two-dimensional mass balance holds. However, Allen and Smith found that off Oregon during summer 1973, this term had the largest magnitude of all of the terms in the linearized longshore momentum equation (see Fig. 8, discussed more fully in Section 6). Furthermore, it was not sig-

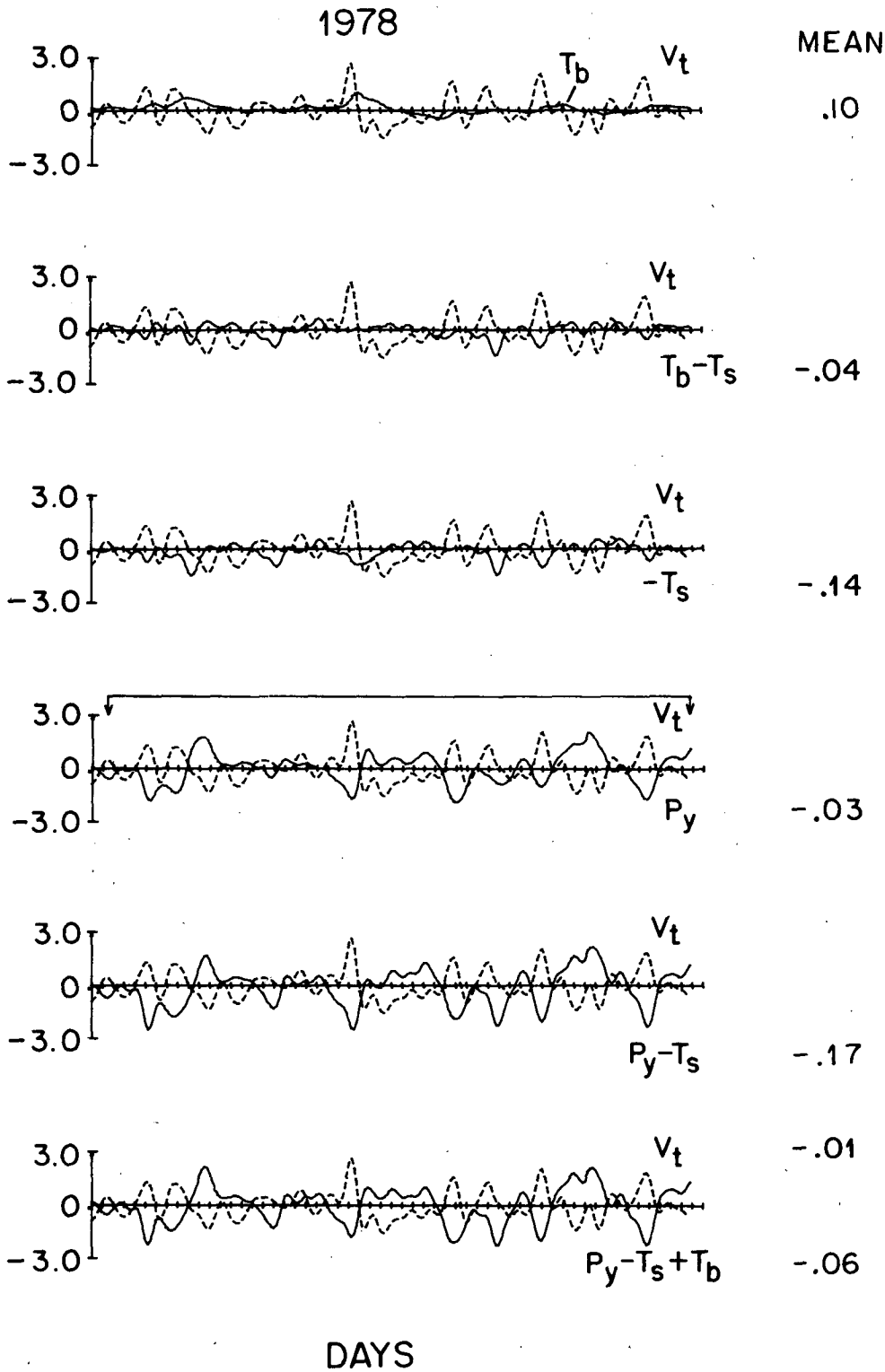

FIG. 2b. As in Fig. 2a but for summer 1978.

nificantly correlated with any of the other variables. The maximum ratio of fU to V_t for a free first-mode hybrid coastal trapped wave in the Pacific Northwest is 15% (D. Battisti, personal communication, 1983 from calculations using the Brink, 1982, model). The present dataset is insufficient to allow calculation of

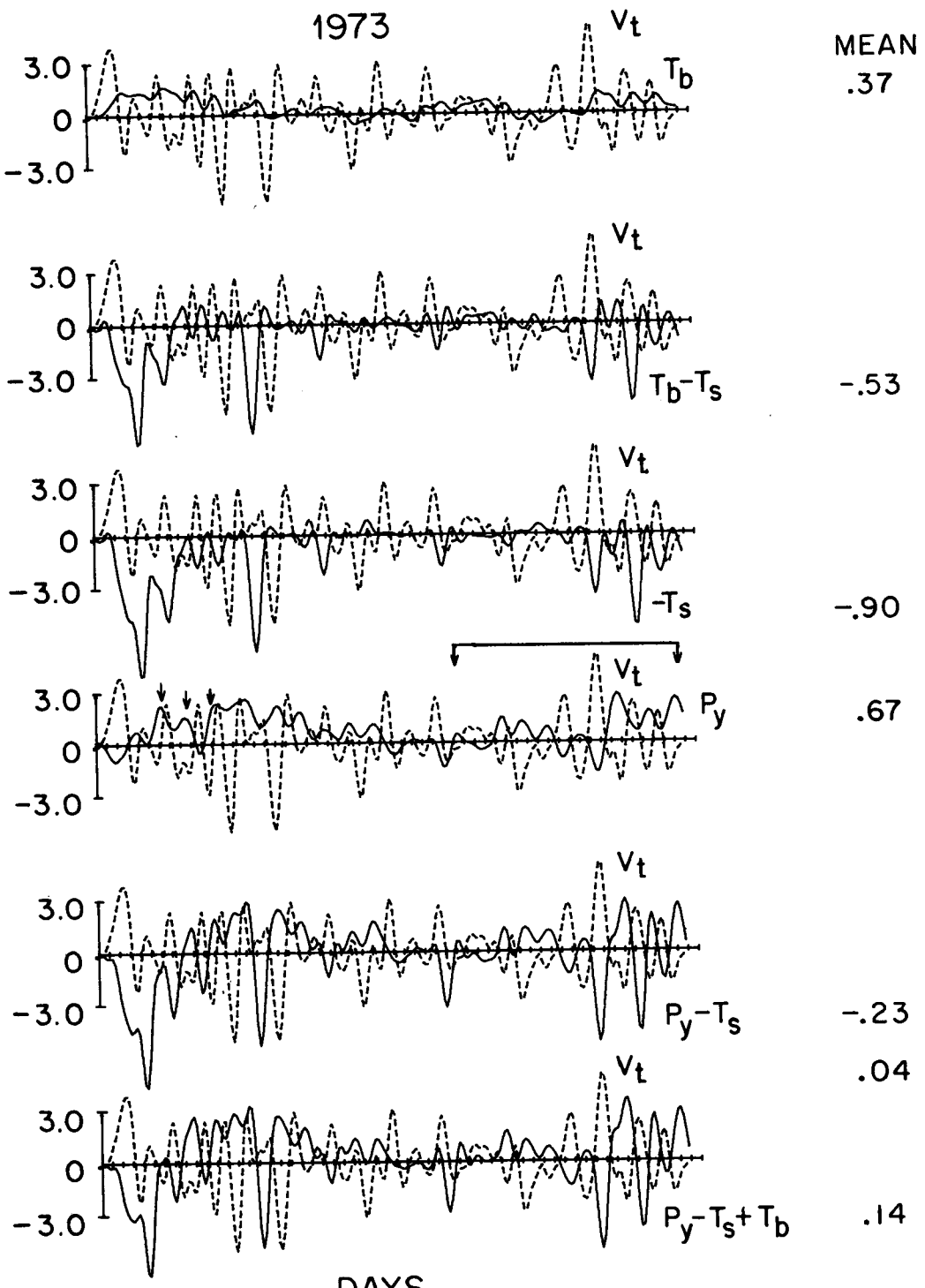

FIG. 2c. As in Fig. 2a but for winter 1973.

fU. However, the remarkable degree of balance obtained between V_t and those momentum terms that can be calculated suggests that the coastal trapped wave estimate is not unreasonable.

4. The balance of momentum

Line plots of individual and combined terms in Eq. (1) (Figs. 2a–d) illustrate the most important result;

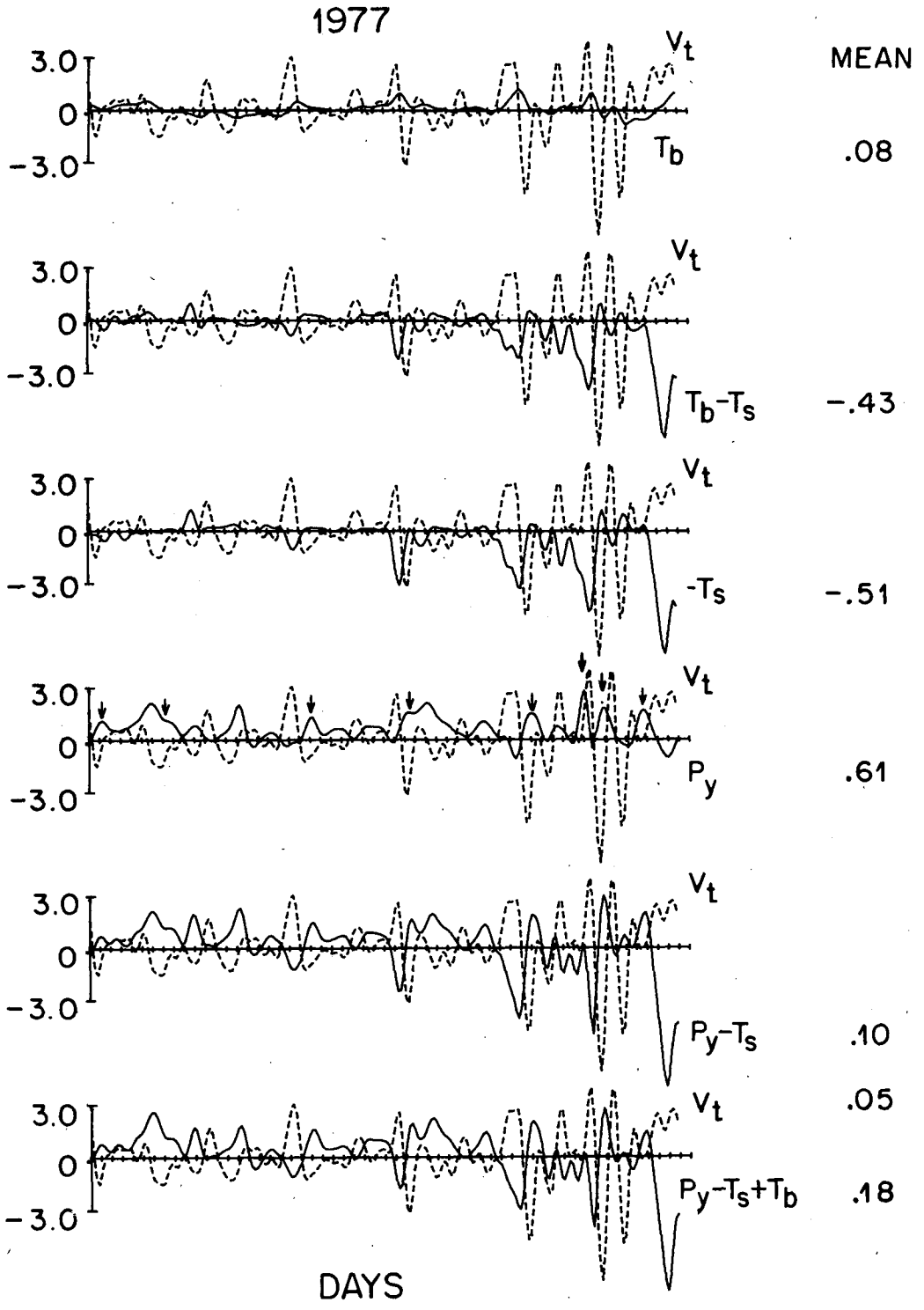

FIG. 2d. As in Fig. 2a but for winter 1977.

i.e., the time series obtained by combining T_s and $-p_y$ balances the observed acceleration V_t better than either T_s or $-p_y$ individually. Events or periods during which p_y appears to be essential to the momentum balance are indicated in the figures. Bottom stress is much smaller than the other terms in the equation of motion. However T_b, when significant, improves the phase relationship between V_t and the sum of the forcing func-

tions. The line plots illustrate that not only the fluctuations, but also the means of the V_t and $p_y - T_s + T_B$ time series are relatively well balanced (compare zero crossings of the two series). The mean of V_t is much less than the mean of both T_s and p_y. Bottom stress provides some fraction of the momentum necessary to balance mean T_s in summer 1978 and in winter 1973. In three of the four records, the principal balance for mean T_s is provided by mean p_y.

Both T_s and $-p_y$ appear to accelerate or decelerate the flow independently. During some extended periods, T_s dominates, e.g., winter 1977, last third of the record. During other periods $-p_y$ dominates, e.g., summer 1978 and winter 1973, for the last third of the record. In a given month, several events may be primarily T_s driven and several others, $-p_y$ driven so that the best balance to V_t during the entire month is obtained by adding T_s and $-p_y$ together.

These results are confirmed by the relative magnitudes of the spectra of individual and combined terms in Eq. (1) (Figs. 3a and b). Surface stress and $T_s - T_b$ have insufficient energy to balance V_t at all but the lowest frequencies (<0.15 cpd). On the other hand, $T_s - p_y$ is closer to the energy of V_t in most frequency bands in all four cases.

Coherence spectra confirm that V_t is generally more coherent with $T_s - p_y$ than with T_s (Figs. 4a and b). The greatest improvement in coherence occurs during summer when V_t is more coherent with $-p_y$ than with T_s at most frequencies. Coherence between all momentum terms in 1973 is significantly lower than that in the other years. The low coherence values are probably due to the first six days and the middle portion of the record; i.e., the end portion looks remarkably like the records in the other years in which $-p_y$ contributes substantially to the acceleration (Fig. 2c). The

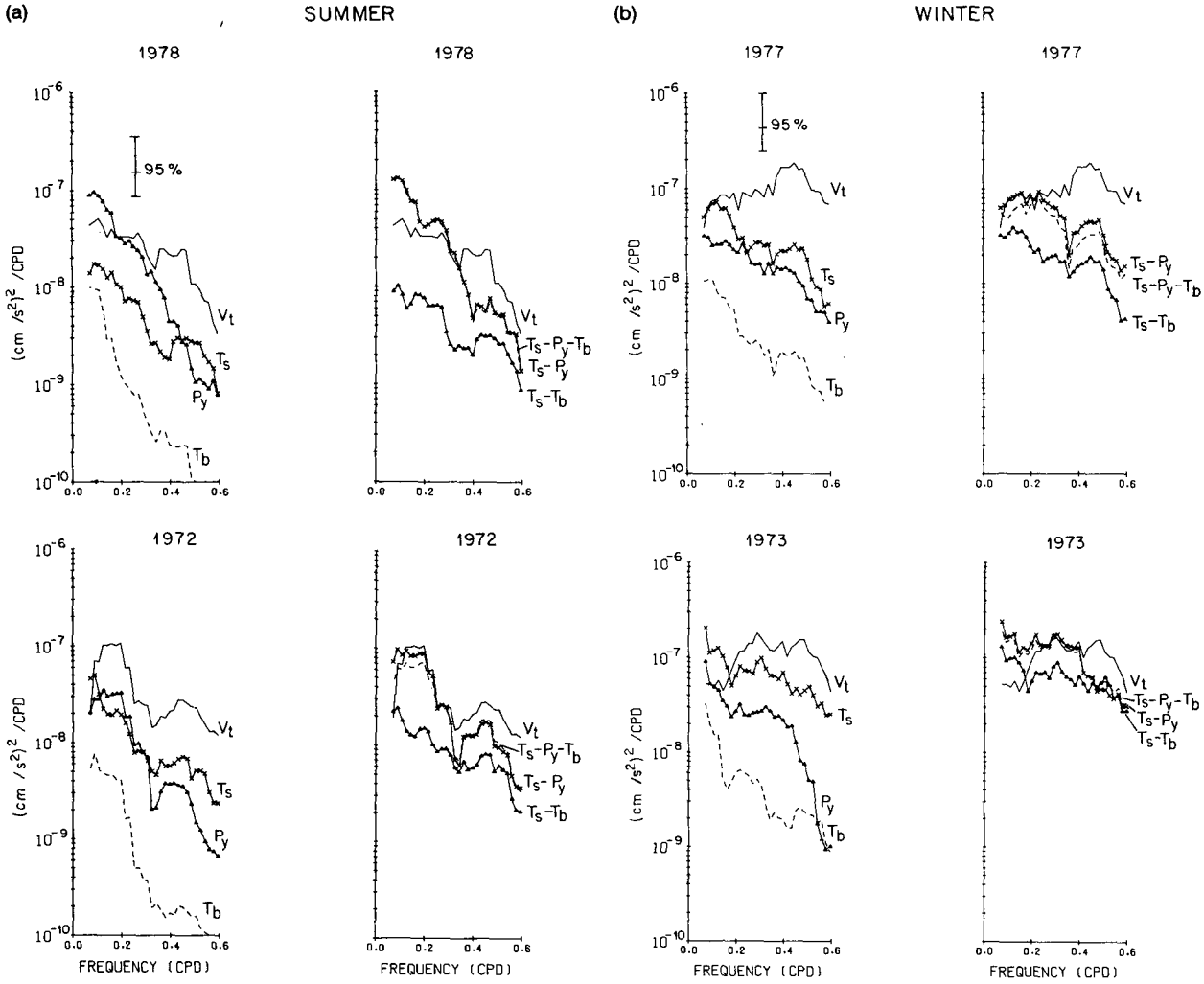

FIG. 3. A comparison for the (a) summer season and (b) winter season of the spectra of individual and combined terms in the vertically averaged longshore momentum equation with the spectrum of acceleration V_t. Record length is 56 days. Each spectral estimate has 14 degrees of freedom.

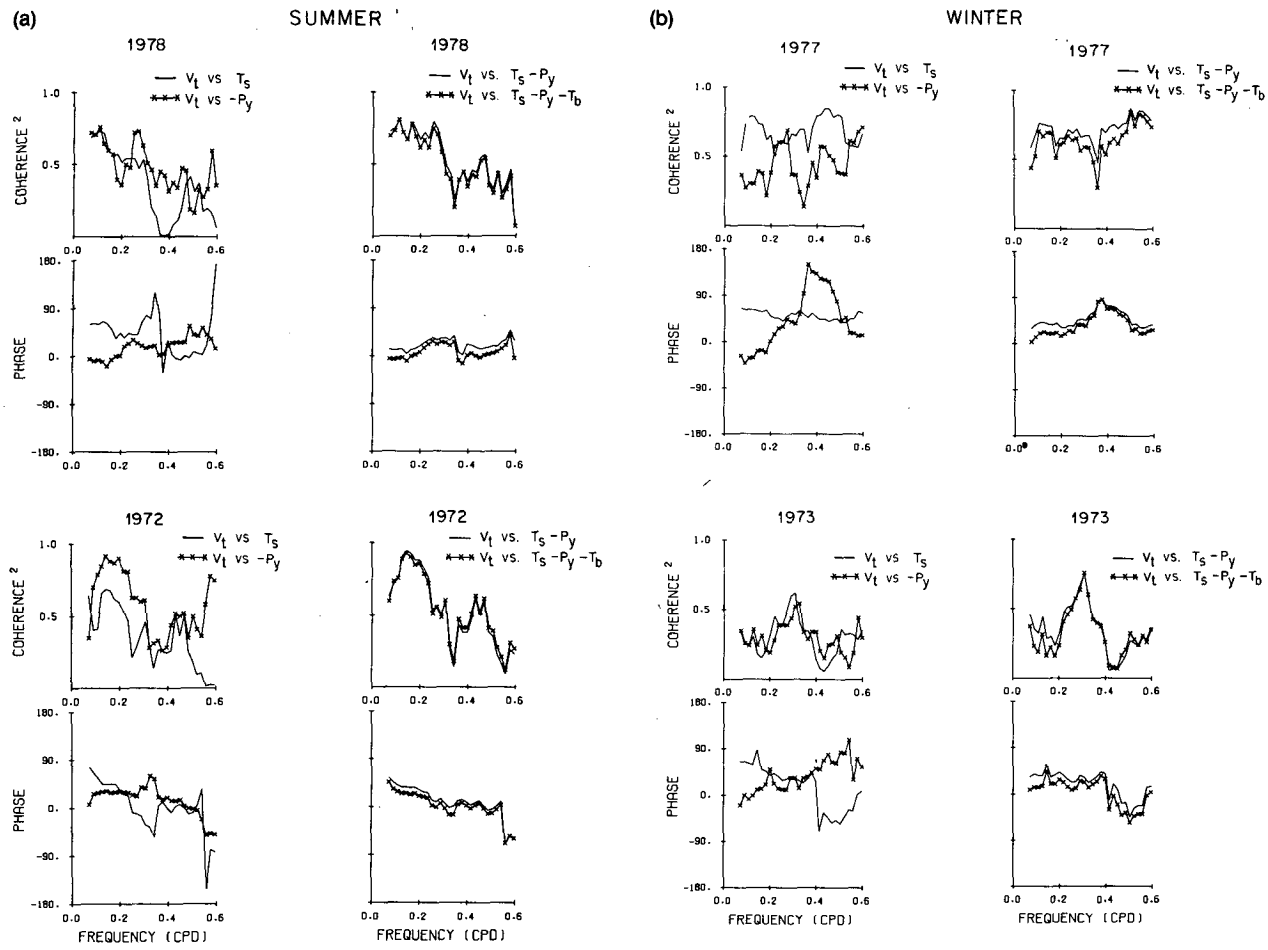

FIG. 4. Coherence squared and phase estimates between acceleration V_t and individual or combined terms in the large-scale vertically averaged longshore momentum equation during (a) summer and (b) winter. A positive phase difference indicates that V_t leads the other series. An estimate of 0.47 is significant at the 95% level (Koopmans, 1974).

line plots suggest that during the first six days, $-p_y$ alone would balance V_t.

Comparison of the phase relationship between V_t and individual and combined forcing functions also suggests that $T_s - p_y$ provides a better balance to the observed acceleration than T_s (Figs. 4a and 4b); the phase difference is closer to zero when $-p_y$ is included. The only exception to this observation occurs in 1977 at frequencies between 0.3 and 0.5 cpd. This deviation from the overall pattern will be discussed further in the next section. Addition of bottom stress to the total forcing function generally results in phase differences even closer to zero.

5. The nature of the forcing and response

The importance of $-p_y$ to the longshore momentum balance suggests that coastal trapped waves may make important contributions to the Pacific Northwest fluctuating velocity field (Allen, 1980). The first mode hybrid coastal trapped wave in the Pacific Northwest is essentially barotropic (Brink, 1982) and has a relatively large longshore scale ($\lambda > 1200$ km for frequencies < 0.3 cpd) so that its associated pressure field should be adequately resolved by the subsurface pressure (i.e., tide gage height plus atmospheric pressure) time series presented herein over most of the event frequency range. In this section the propagation characteristics and scales of the wind, pressure and pressure gradient fields and their relationship to each other and to V_t are examined in the context of wave models, utilizing the present dataset. A complete examination of the forced wave response in the Pacific Northwest to coastal wind forcing along the entire west coast during these time periods has been submitted as a separate paper (with D. Battisti).

Wave models suggest that the longshore component of wind stress all along the west coast contributes to the longshore coastal pressure field (Clarke, 1977). In a region where local wind forcing is not significant, the pressure signal propagates northward through that region at the free wave speed (for a given mode). In

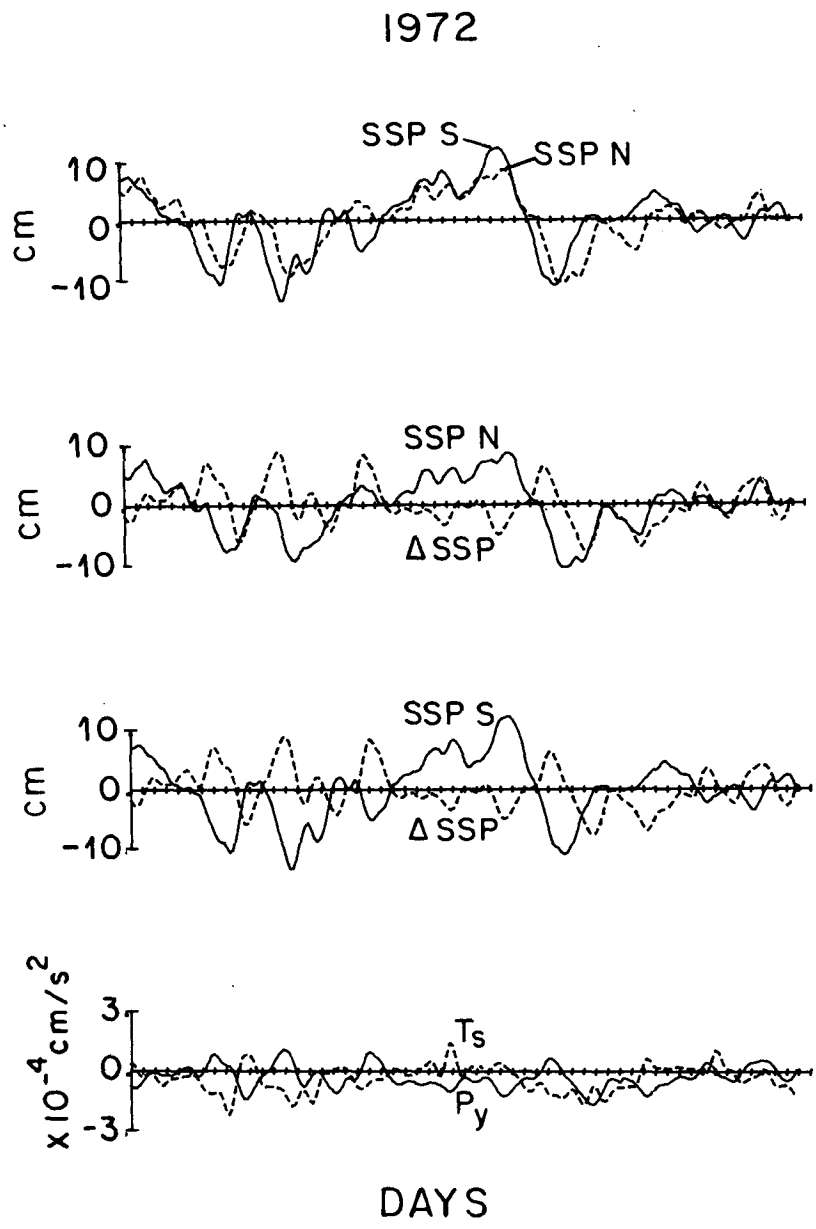

FIG. 5a. Time series of SSP (means removed) at locations separated alongshore by 420 km during summer 1972. N represents Neah Bay, Washington and S represents South Beach, Oregon, the tide gauge stations; T_s, p_y and the pressure difference, ΔSSP (north minus south), are also shown. The top panel illustrates the northward propagation of SSP signals and the similarity (or lack of similarity) of the signals alongshore. The middle two panels illustrate the relationship between ΔSSP and SSP at the north and south stations. The bottom panel illustrates the relationship between T_s and p_y.

general, a sum of modes, each of which has a characteristic phase speed, could be present. If local forcing is significant in a region, the longshore phase characteristics of the pressure field are a function of the propagation characteristics of the local wind field as well as a function of the freely propagating wave field. In the Pacific Northwest, the wind field appears to travel northward during summer and to travel at least as rapidly as a free first mode shelf wave (Huyer *et al.*, 1975, for summer 1972; Wang and Mooers, 1977, for summer 1973). During winter, the one available study that uses measured winds suggests that wind forcing is essentially simultaneous over the Pacific Northwest (Hickey, 1981). This result is confirmed by large-scale (3° grid) wind stress data computed from widely spaced atmospheric pressure data for 1967–73 (Bakun, 1975).

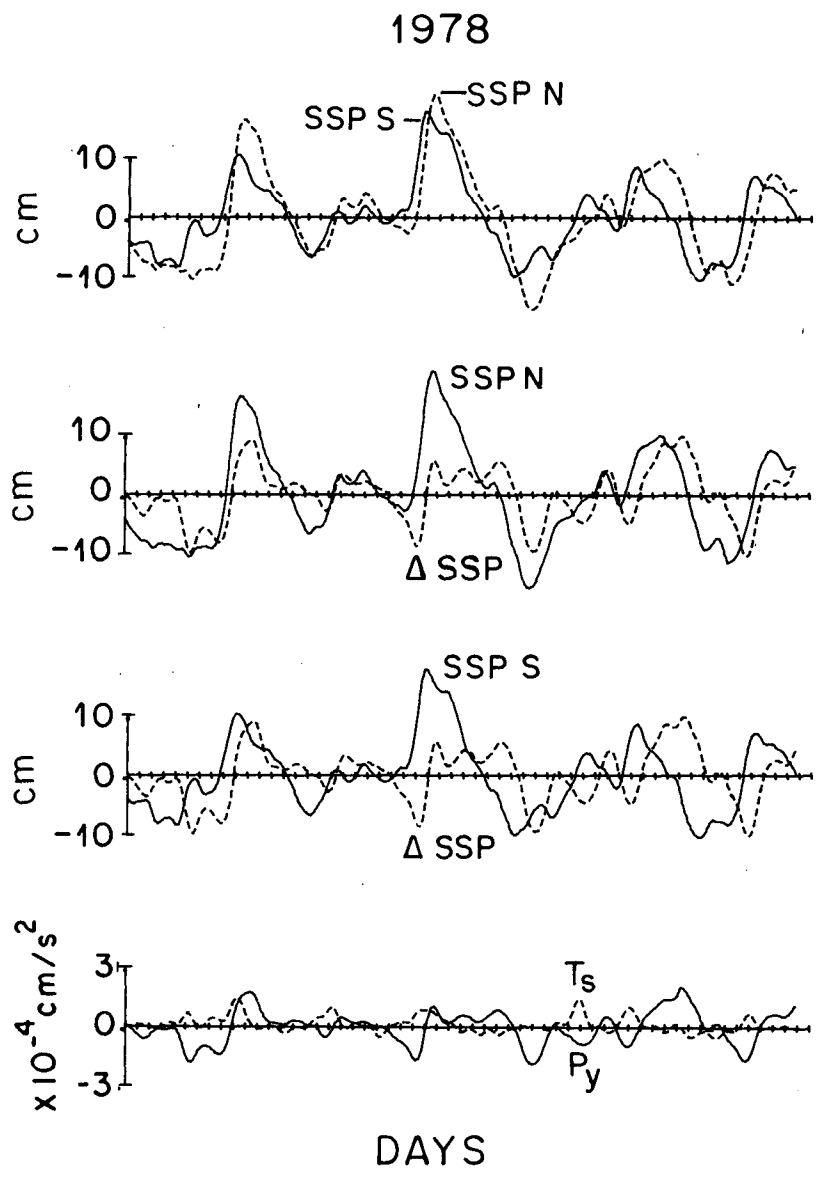

FIG. 5b. As in Fig. 5a but for summer 1978.

Superposition of subsurface pressure (SSP) time series from the northern and southern stations illustrates dramatically the northward propagation of the majority of the signals (Figs. 5a–d). The northward propagation is most apparent whenever local wind stress is weak, for example, most of summer 1978; winter 1977, for the first two-thirds of the record. During such periods, south to north lags on the order of a day, consistent with the propagation of a free first mode wave for this region (490 cm s^{-1}, Brink, 1982), are plainly evident in the records. Conversely during strong local wind events, such as occur during winter 1973 in the first third of the record and winter 1977 in the last third, the apparent south to north phase lag is often reduced, as expected.

The impact of local forcing on the statistics of phase characteristics calculated over any two month period is significant. Lower frequency (~0.1 cpd) signals, which are significantly coherent alongshore in all four records, appear to travel slightly faster during summer (560 and 710 cm s^{-1} for 1972 and 1978) than a free first mode shelf wave and more than twice the free wave speed during winter (1090 and 1350 cm s^{-1} for 1973 and 1977) (Fig. 6). Phase differences for frequencies in the range 0.20–0.35 cpd are also consistent with propagation at speeds faster than that of a free first-mode shelf wave in this region, and the apparent propagation (for coherence squared significant at the 95% level) is also faster during winter than during summer.

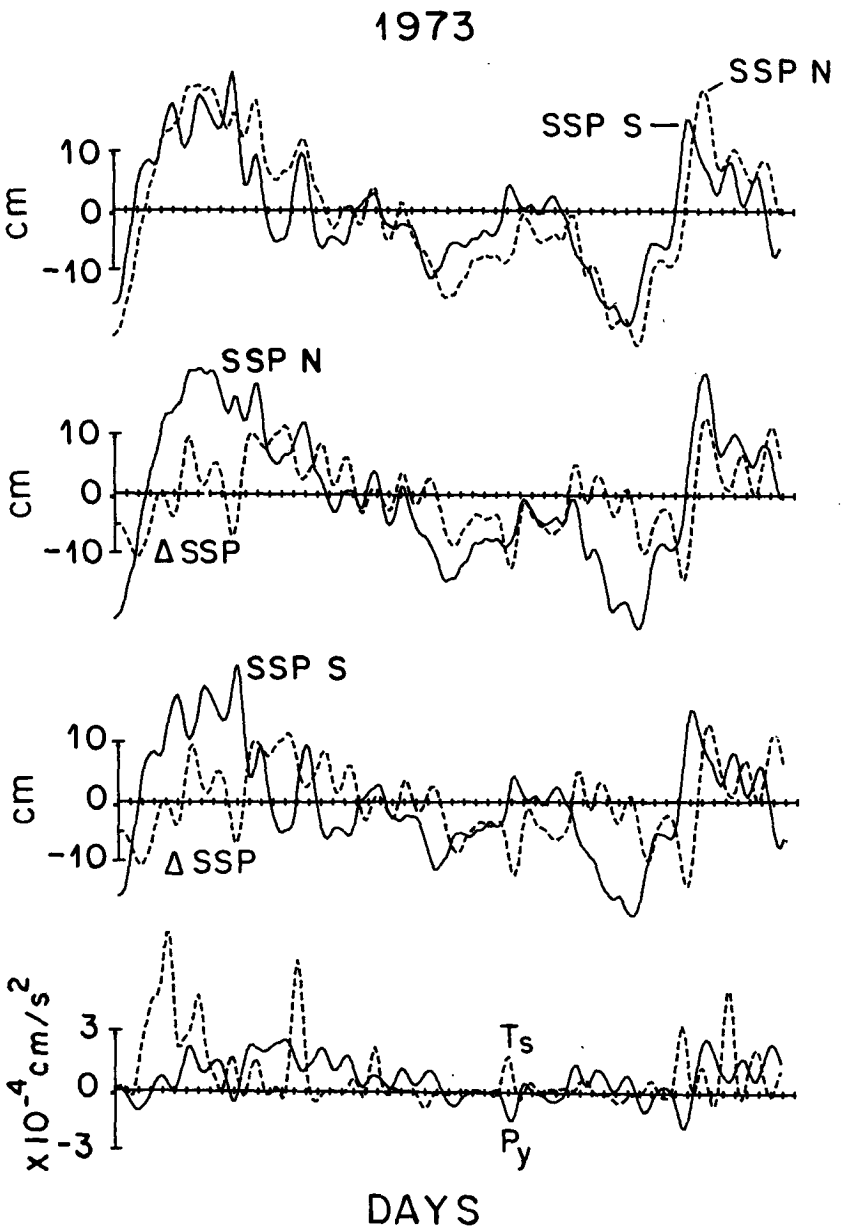

FIG. 5c. As in Fig. 5a but for winter 1973.

Comparison of the SSP signals with the longshore pressure difference, ΔSSP, demonstrates that p_y has the characteristics expected for a traveling wave: it is not simply the image or mirror image of one signal at one or the other location (Figs. 5a–d). The difference in phase information of p_y relative to SSP is illustrated in Fig. 7. The phase difference between V_t and $-p_y$ at frequencies for which coherence squared was significant at the 50% level is close to zero, as might be expected for a free coastal trapped wave response for which fU is relatively small (Allen, 1980; Mysak, 1980). The average phase difference between V_t and SSP at the northern and southern stations, on the other hand, generally approaches 90° as expected for cross-stream geostrophic balance.

An exception to the above conclusion occurs in 1977 at frequencies between 0.3 and 0.5 cpd. In this band the alongshore coherence of the pressure signals drops to zero (Fig. 6) and the phase relationship between V_t and SSP at the southern station is identical to that between V_t and $-p_y$. This may explain why the phase difference between V_t and $T_s - p_y$ in this band has a significantly different pattern from the other cases considered, as previously mentioned. It appears that at the higher frequencies during at least this one winter, p_y has not been adequately resolved.

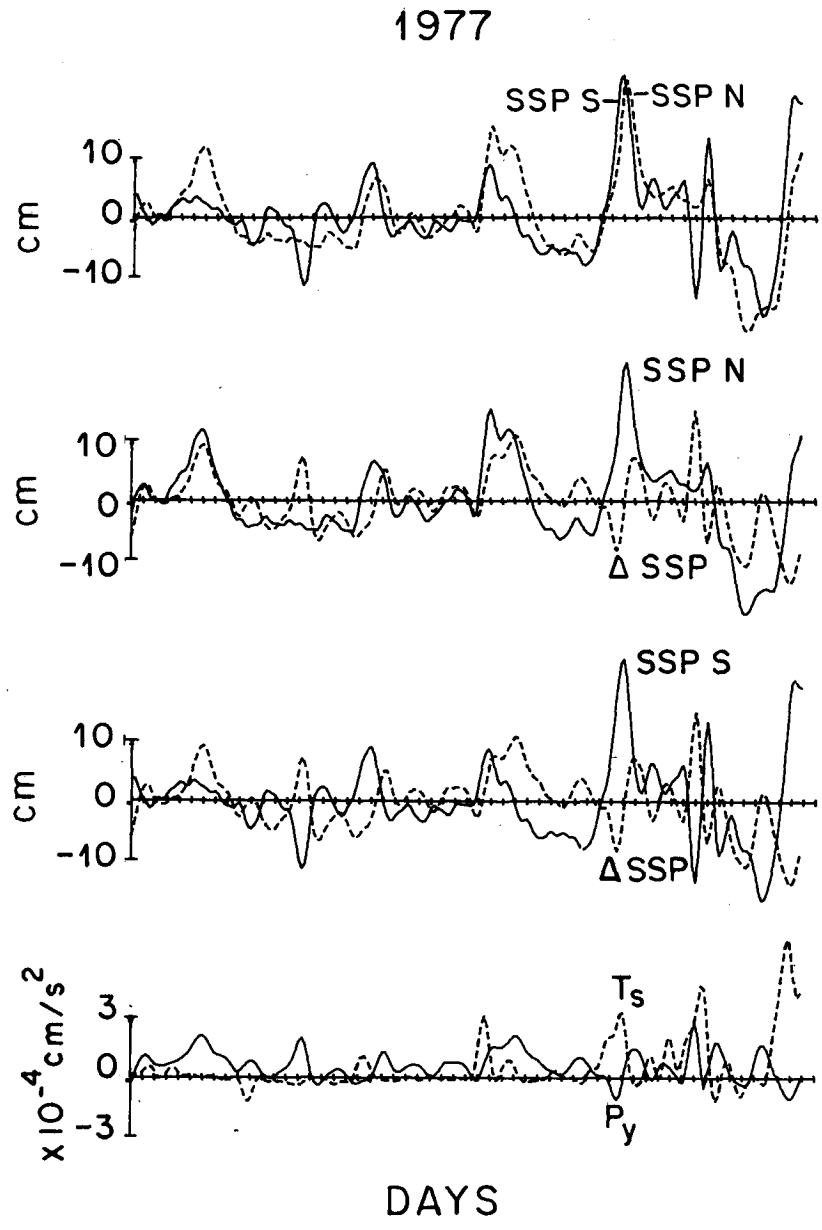

FIG. 5d. As in Fig. 5a but for winter 1977.

The large wavelengths defined by the SSP field for the lower frequency bands explain why the pressure differences are adequately resolved by the 420 km sea level station spacing. Acceleration and currents estimated midway between SSP stations, as in 1972, 1973 and 1977, should have roughly the correct phase to match p_y (for small T_b and T_s). In 1978, when acceleration was almost entirely driven by p_y, the measurements of V_t were located near the southern SSP station. However, the low frequency (<0.2 cpd) fluctuations had a very large wavelength (5590 km) so that the relative locations of the velocity and pressure stations did not result in a significant phase difference between V_t and p_y. In the band 0.25–0.35 cpd, for which the computed wavelength of the signal was 2070 km, V_t leads $-p_y$ slightly, as would be expected.

Although τ_s and $-p_y$ can independently accelerate the water column [via Eq. (1)], τ_s and p_y are not, in general, independent functions. For example, if the pressure field is primarily a response to coastal trapped waves, p_y would be determined by τ_s all along the coast as previously mentioned. Contributions to the gradient at a specific location from other locations would be primarily a function of longshore variations in τ_s, longshore variations in topography and the degree of frictional damping. Coherence of the local value of p_y with local τ_s would be a function of the longshore scale of the wind disturbances. The observations suggest that

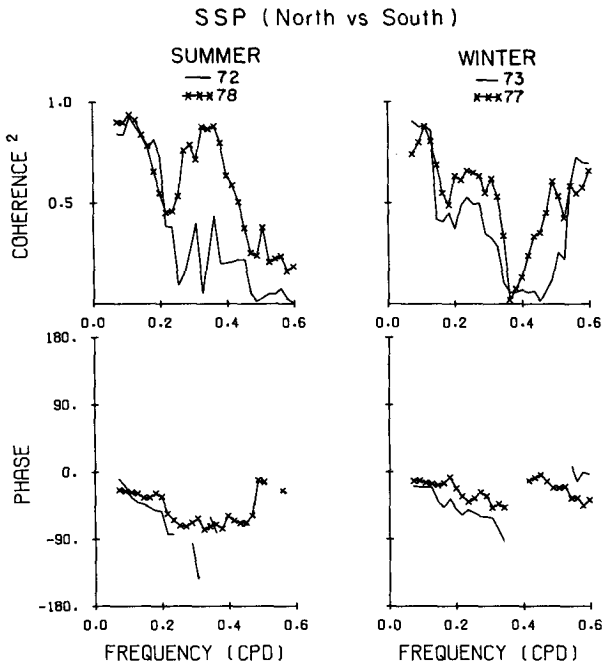

FIG. 6. Coherence squared and phase estimates between time series of SSP separated alongshore by 420 km. A negative phase difference indicates northward propagation. A coherence squared of 0.47 is significant at the 95% level (Koopmans, 1974). Phase estimates are shown only for coherence squared values that exceed the 50% significance level (0.23).

local τ_s and the local value of p_y are only weakly related (Fig. 8). In cases where the coherence is significant at the 95% level, the phase difference generally approaches closer to zero than to the 180° expected for a setup type of response as suggested by Allen and Smith (1981) for summer 1973 (see also the line plots in Figs. 5a–d, bottom panel). These relationships suggest that contributions to the Pacific Northwest pressure field from locations south of the Pacific Northwest (i.e., remotely forced contributions) must be significant.

6. Discussion

These results when presented at the Fall 1982 AGU Meeting in San Francisco, and at the joint United States–Australian 1982 workshop in Asilomar generated considerable debate. The principal question centered on the disagreement with the Allen and Smith (1981) results that are shown in Fig. 9. They found a positive correlation between p_y and T_s; also, V_t and p_y were positively correlated rather than negatively correlated as demonstrated herein. Moreover, T_s, which was obtained from *in situ* wind measurements, was too small to balance V_t. Their tide gauge stations were ~100 km apart whereas those in this study were ~420 km apart, suggesting that local topography and/or smaller scale processes may have significant effects on the response of individual tide gauge stations. Results shown herein suggest that the 420 km station spacing used and the particular stations selected are generally adequate to define longshore pressure gradient perturbations in this region at frequencies at least as high as 0.3 cpd.

The general results obtained in this study are relatively insensitive to the amplitudes of both wind stress and pressure gradient data. Attempts to improve the "fit" produced some changes in the appearance of the line plots (Figs. 2a–d), but had relatively minor effect on coherences and phases. Fig. 10 illustrates the effect of including a land-to-ocean wind gradient for one winter and one summer case. The correlation between V_t and $T_s - p_y$ is essentially the same whether or not the gradient is included, but the amplitudes are somewhat better matched during winter with the larger wind stress. However, the energy levels during summer 1972 are mismatched with the larger wind stress. This apparent discrepancy is explained by the fact that the seasonal mean longshore wind stress decreases by a factor of 2 between Oregon and Washington during

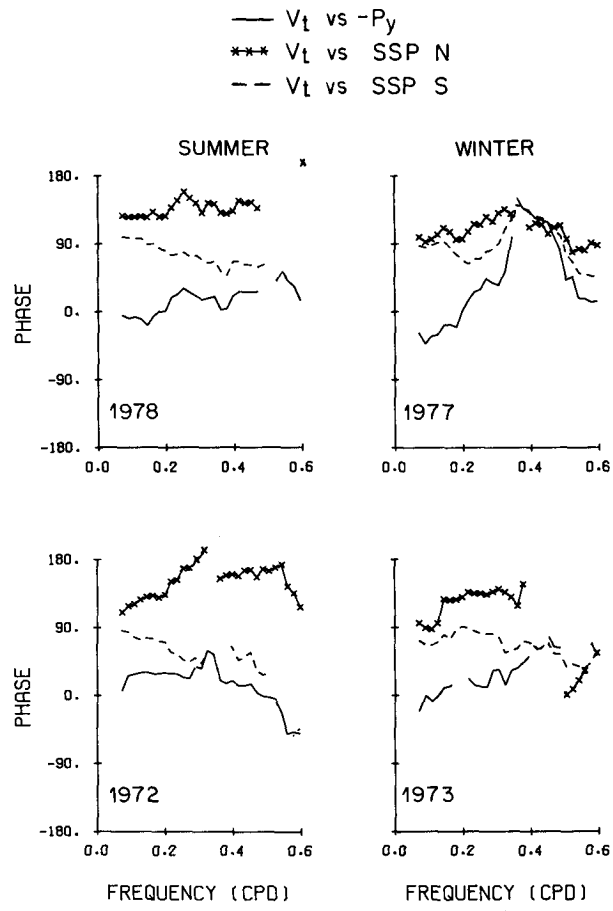

FIG. 7. Phase estimates between V_t and $-p_y$, V_t and SSP at South Beach (S) and V_t and SSP at Neah Bay (N). A positive phase difference indicates that V_t leads the other parameters. Phases are given only for coherence squared values that are significant at the 50% level.

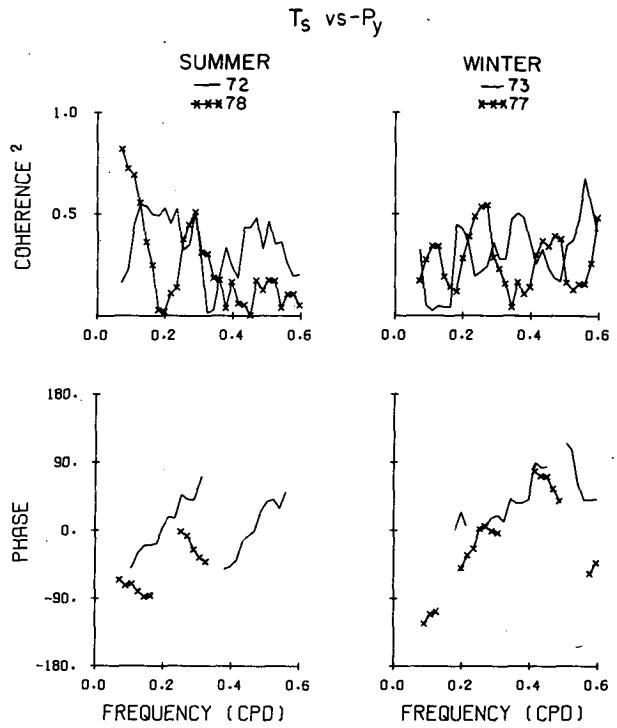

FIG. 8. Coherence squared and phase estimates between T_s and $-p_y$. A positive phase difference indicates that T_s leads $-p_y$. An estimate of 0.47 is significant at the 95% level (Koopmans, 1974). Phases are given only for coherence squared values that are significant at the 50% level.

summer (Nelson, 1977), roughly balancing the land-to-ocean increase off Newport.

The general results are sensitive to the depth selected to represent the vertical average of the water column; namely, tests indicate that near-surface data are contaminated by eddy activity (Fig. 11). The midshelf longshore pressure gradient associated with the generally small-scale (~40 km) eddies that are common on this coast cannot be resolved by a sea level network that consists of coastal tide gauges separated by at least 400 km. The results suggest that single depth data below the depth of near-surface eddies may provide a better estimate of the large-scale acceleration than a vertical average of the entire water column.

The results of this study are also sensitive to the contribution of the monthly mean pressure gradient to the momentum balance. During winter, the mean pressure gradient is on the order of 50% of the amplitude of the fluctuating pressure gradient. While this contribution does not affect energy levels and coherences, it does affect the instantaneous balance of momentum; the zero crossings in the line plots in Figs. 2a–d would not match without inclusion of the mean pressure gradient. In all cases except 1978 (for which both mean T_s and mean p_y were relatively small), the mean pressure gradient is necessary to balance the mean wind stress.

7. Conceptual framework for Pacific Northwest coastal dynamics

The momentum balance results for summers 1972 and 1978 and winters 1973 and 1977 exhibit significant seasonal and interannual variability. Monthly mean wind stress anomalies (seasonal cycle removed) indicate that summer 1978 was a case of anomalously strong stress; both winters were examples of anomalously weak wind stress and 1977 had weaker stress than 1973 (Pittock *et al.*, 1982). Wind and V_t data from 1975, a case of slightly stronger than average winter stress, are included in the interannual comparison of acceleration and forcing functions given in Figs. 12a–c. Examination of the seasonal and interannual variability of the results of the present analysis in conjunction with results reported in the literature for other

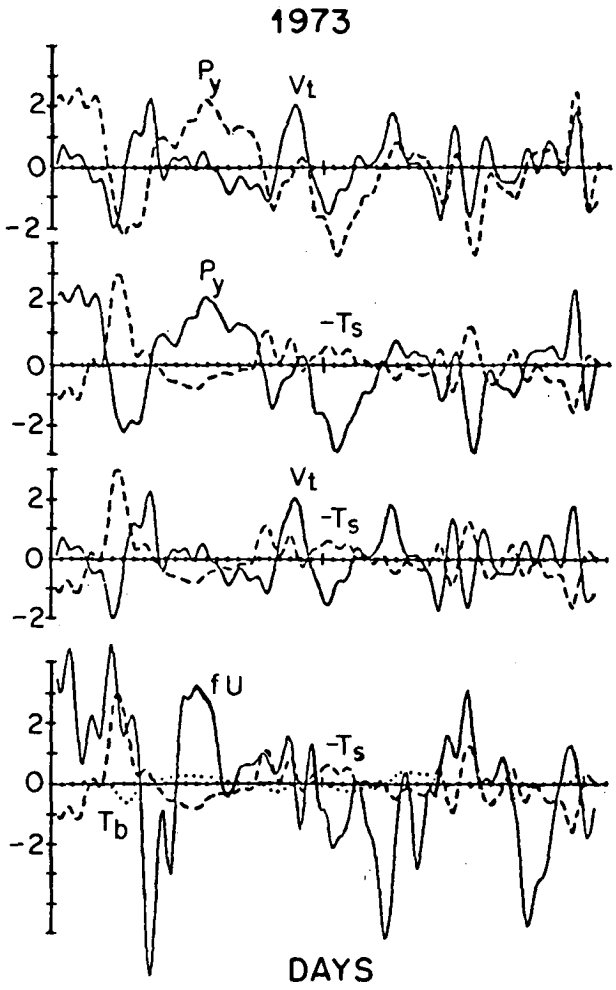

FIG. 9. Principal terms in the vertically averaged longshore momentum equation (with means removed) for Oregon in summer 1973 (taken from Allen and Smith, 1981). Units are 10^{-4} cm s^{-2}. A mirror image between a pair of plots indicates a perfect balance of momentum. Note the difference in sign between the P_y, V_t relationship in this figure and that in Fig. 2b for summer 1978.

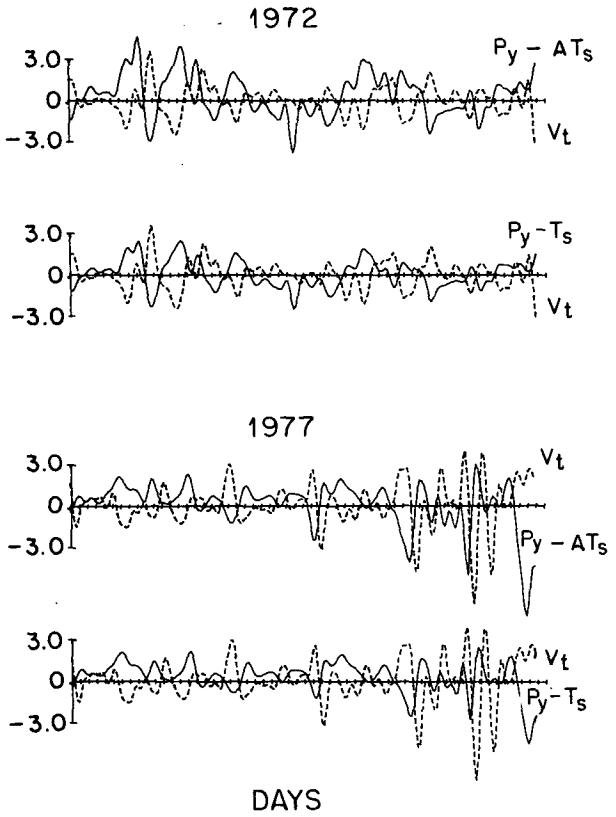

FIG. 10. Comparison of time series of V_t and forcing functions with and without the coast-to-ocean gradient in wind speed. The cases with amplified wind data are indicated in the figure as $p_y - AT_s$. Units are 10^{-4} cm s^{-2}.

time periods, allows the beginnings of the development of a conceptual framework for understanding the relative importance of various large-scale processes in the Pacific Northwest during any particular period. The following framework is presented as a summary of the most significant dynamical results of this paper.

1) At low frequencies (0.1–0.3 cpd), remotely generated freely propagating first mode coastal trapped waves appear to make important contributions to Pacific Northwest longshore current fluctuations during all periods. This result is based on statistical demonstration of a wave-like momentum balance ($V_t = -p_y$) consistent with the essentially barotropic nature of the free first mode coastal trapped wave in this region, apparent alongshore propagation speeds of 100–300% of the first mode free wave speed and last, a weak relationship between local τ_s and p_y.

2) The relative contribution of local wind stress ($T_s = \tau_s/H$) and the propagating wave field (p_y) to the local acceleration appears to be dominated by the contribution of local T_s; i.e., T_s exhibits much more interannual variability than p_y (Figs. 12b,c and Fig. 12d) which gives the ratio of T_s to p_y). One possible explanation for this result is that if the pressure gradient field in the Pacific Northwest is the cumulative response to wind driving all along the coast, the effect of interannual longshore variations in locations of the atmospheric high or low pressure (which determines the longshore coastal wind field) will be smoothed to some degree by the integration. Thus, the local momentum balance appears more free-wave-like in the weak local wind summer 1978 case ($T_s/p_y \sim 0.5$ in the band 0.1–0.4 cpd) than in the strong local wind summer 1972 case ($T_s/p_y \sim 1.7$ in the band 0.1–0.4 cpd), which has been described as a case of resonant wave forcing (Kundu and Allen, 1976). Similarly, during winter the most significant wave-like contributions ($T_s/p_y < 1.5$ over most of the low frequency band) are observed during the weakest local wind case (1977). The closer to average (slightly strong) local wind case (1975) has been described as one of purely local wind forcing (Hickey, 1981).

3) At high frequencies (0.35–0.50 cpd) during winter, first mode freely propagating coastal trapped waves do not appear to be as important to the fluctuating current field. This result is based on the extremely rapid (cf. the first mode free wave) alongshore propagation of the SSP signal in one case and the occurrence in this band of near-zero alongshore coherence of the SSP signals over the 420 km station spacing for both cases. However, the largest acceleration fluctuations are usually excited in this band during winter; winter and summer acceleration spectra are strikingly different in this respect (Fig. 12c). The interannual variability of T_s in this band is at least a factor of 5 (amplitude^2) greater than that of V_t during both summer and winter; also, in two out of three winters and both summers T_s as estimated herein has insufficient energy to balance

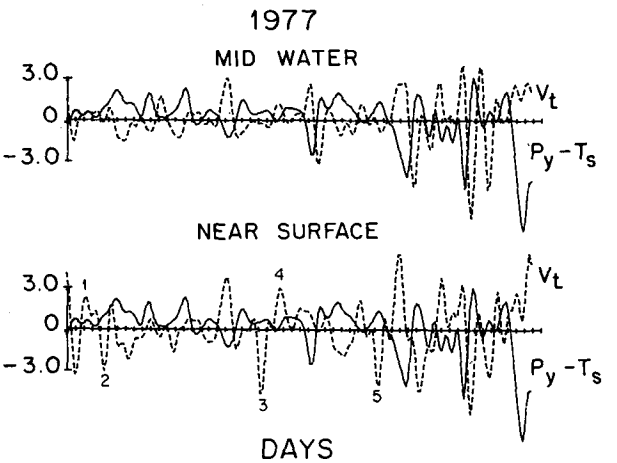

FIG. 11. Principal terms in the vertically averaged longshore momentum equation as a function of time during winter 1977. Units are 10^{-4} cm s^{-2}. Longshore acceleration V_t has been computed from both near-surface (25 m) and mid-water column (80 m) data. A mirror image between a pair of plots indicates a perfect balance of momentum. Numbers indicate possible near-surface eddy activity.

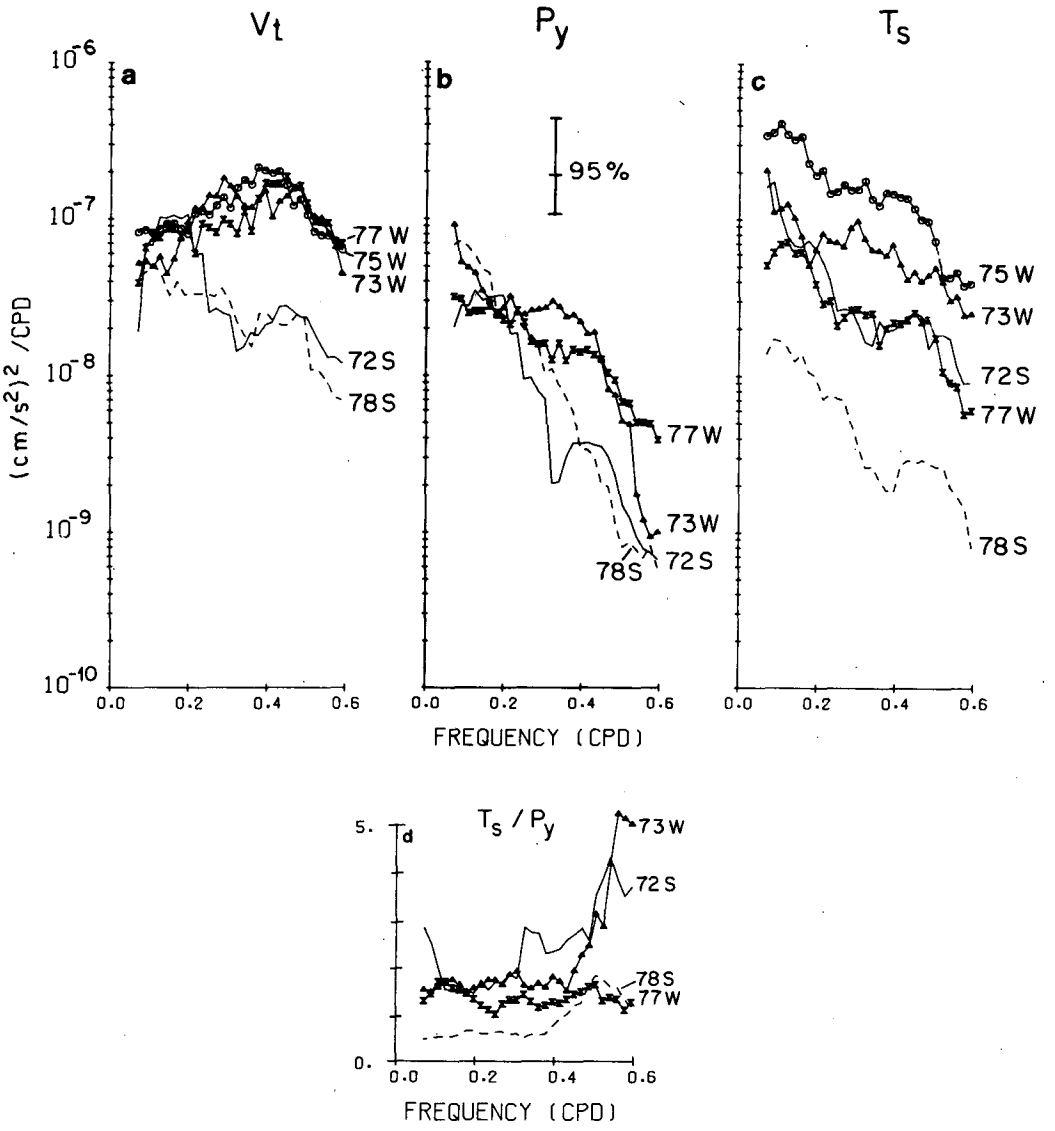

FIG. 12. Spectra of (a) V_t, (b) p_y and (c) T_s in various years. Data from winter 1975 begin on 11 January. These data are at a depth of 47 m from the surface near the winter 1977 location (bottom depth 7 m shallower, 3 km south of 1977 location). Each record length is 56 days. Spectral estimates have 14 degrees of freedom. The square root of the ratio of the spectral amplitudes of T_s and p_y is given in (d). Newport wind data were used for all stress computations and in every case, the wind was multiplied by a factor of 1.3 to simulate the coast-to-ocean gradient in wind speed. Estimates of p_y were multiplied in each case by an offshore decay factor of 0.7.

V_t in this band. Although p_y may be important, at least one p_y record estimated from the tide gauges at 420 km longshore spacing appears to contain noise at these frequencies. The forcing of the most energetic winter fluctuations remain at this time an unresolved and intriguing problem.

Acknowledgments. I would like to thank Dr. Adriana Huyer and Dr. Robert L. Smith at Oregon State University for their generous contribution of the Newport wind data and of the South Beach sea level and atmospheric pressure data. Marco Venturi assisted in initial exploration of the dataset. A special thanks is extended to Susan Geier, who performed the calculations contained herein with her usual care and enthusiasm. The current meter data were collected with AEC support under Contract AT(45-1)-2225 (1972 and 1973) with DOE support under Contract EY-76-S-06-2225 TA25 (1975 and 1977) and with NSF support under Grant OCE 77-08791 (1978, as part of the Poleward Undercurrent Experiment executed jointly with Huyer and Smith). The analysis was supported by the Department of Energy under Contract DE-AT06-76-EV-71025 and by the National Science Foundation under Grant OCE 80-23465.

REFERENCES

Allen, J. S., 1980: Models of wind-driven currents on the continental shelf. *Ann. Rev. Fluid Mech.*, **12**, 89–433.

——, and R. L. Smith, 1981: On the dynamics of wind-driven shelf currents. *Phil. Trans. Roy. Soc. London*, **A302**, 617–634.

Bakun, A., 1975: Daily and weekly upwelling indices, West Coast of North America 1967–73. NOAA Tech. Rep. NMFS SSRF-693, 114 pp.

Brink, K. H., 1982: A comparison of long coastal trapped wave theory with observations off Peru. *J. Phys. Oceanogr.*, **12**, 897–913.

Clarke, A., 1977: Observational and numerical evidence for wind-forced coastal trapped long waves. *J. Phys. Oceanogr.*, **7**, 231–247.

Enfield, D. B., and J. S. Allen, 1980: On the structure and dynamics of monthly sea level anomalies along the Pacific coast of North and South America. *J. Phys. Oceanogr.*, **10**, 557–578.

Halpern, D., 1976: Measurements of near-surface wind stress over an upwelling region near the Oregon coast. *J. Phys. Oceanogr.*, **6**, 108–112.

Hickey, B. M., 1981: Alongshore coherence on the Pacific Northwest continental shelf (January–April, 1975). *J. Phys. Oceanogr.*, **11**, 822–835.

——, and N. Pola, 1983: The seasonal alongshore pressure gradient on the west coast of the United States. *J. Geophys. Res.*, **88**, 7623–7633.

Huyer, A., B. M. Hickey, J. D. Smith, R. L. Smith and R. D. Pillsbury, 1975: Alongshore coherence at low frequencies in currents observed over the continental shelf off Oregon and Washington. *J. Geophys. Res.*, **80**, 3495–3505.

——, R. L. Smith and E. Sobey, 1978: Seasonal differences in low-frequency current fluctuations over the Oregon continental shelf. *J. Geophys. Res.*, **83**, 5076–5089.

Kachel, N., 1980: A time dependent model of sediment transport and strata formation on a continental shelf. Ph.D. thesis, School of Oceanography, University of Washington, 123 pp.

Koopmans, L. H., 1974: *The Spectral Analysis of Time Series*. Academic Press, 366 pp.

Kundu, P. K., 1977: On the importance of friction in two typical continental waters: off Oregon and Spanish Sahara. *Bottom Turbulence, 8th Liege Colloq. Ocean Hydrodyn, 1976*, J. C. J. Nihoul, Ed., Amsterdam, Elsevier, 187–207.

——, and J. S. Allen, 1976: Some three-dimensional characteristics of the low-frequency current fluctuations near the Pacific coast. *J. Phys. Oceanogr.*, **6**, 181–199.

——, —— and R. L. Smith, 1975: Modal decomposition of the velocity field near the Oregon coast. *J. Phys. Oceanogr.*, **5**, 683–704.

Large, W. G., and S. Pond, 1981: Open ocean momentum flux measurements in moderate to strong winds. *J. Phys. Oceanogr.*, **11**, 324–336.

Mysak, L. A., 1980: Recent advances in shelf wave dynamics. *Rev. Geophys. Space Phys.*, **18**, 211–241.

Nelson, C. S., 1977: Wind stress and wind stress curl over the California Current. NOAA Tech. Rep. NMF SSSRF-714, US Dept. of Commerce, 89 pp.

Pittock, H. L., W. E. Gilbert, A. Huyer and R. L. Smith, 1982: Observations of sea level, wind and atmospheric pressure at Newport, Oregon, 1967–1980. Oregon State University Data Rep. No. 98, 158 pp.

Reid, J. L., Jr., and A. W. Mantyla, 1976: The effect of the geostrophic flow upon coastal sea elevations in the northern North Pacific Ocean. *J. Geophys. Res.*, **81**, 3100–3110.

Smith, J. D., B. M. Hickey and J. Beck, 1976: Observations from moored current meters on the Washington continental shelf from February 1971–February 1974. Department of Oceanography, University of Washington, Special Rep. No. 65, 383 pp.

Smith, R. L., 1974: A description of current, wind, and sea level variations during coastal upwelling off the Oregon coast, July–August 1972. *J. Geophys. Res.*, **79**, 435–443.

Wang, D. P., and C. N. K. Mooers, 1977: Long coastal trapped waves off the west coast of the United States, summer 1973. *J. Phys. Oceanogr.*, **7**, 856–864.